Journal of Sound and Vibration 329 (2010) 3660–3678

Contents lists available at ScienceDirect

Journal of Sound and Vibration

journal homepage: www.elsevier.com/locate/jsvi

Polynomial chaos expansions for optimal control of nonlinear random oscillators

Yong-Bo Peng [a,b], Roger Ghanem [b,*], Jie Li [c,d]

[a] Shanghai Institute of Disaster Prevention and Relief, Tongji University, Shanghai 200092, China
[b] Department of Civil and Environmental Engineering, University of Southern California, Los Angeles, CA 90089, USA
[c] School of Civil Engineering, Tongji University, Shanghai 200092, China
[d] State Key Laboratory of Disaster Reduction in Civil Engineering, Tongji University, Shanghai 200092, China

ARTICLE INFO

Article history:
Received 3 September 2009
Received in revised form
1 February 2010
Accepted 16 March 2010
Handling Editor: J. Lam
Available online 18 April 2010

ABSTRACT

The polynomial chaos decomposition of stochastic variables and processes is implemented in conjunction with optimal polynomial control of nonlinear dynamical systems. The procedure is demonstrated on a base-excited system whereby ground motion is modeled as a stochastic process with a specified correlation function and is approximated by its Karhunen–Loeve expansion. An adaptive scheme for stochastic approximation with polynomial chaos bases is proposed which is based on a displacement–velocity norm and is applied to the identification of phase orbits of nonlinear oscillators. This approximation is then integrated in the design of an optimal polynomial controller, allowing for the efficient estimation of statistics and probability density functions of quantities of interest. Numerical investigations are carried out employing the polynomial chaos expansions and the Lyapunov asymptotic stability condition based control policy. The results reveal that the performance, as gaged by probabilistic quantities of interest, of the controlled oscillators is greatly improved. A comparative study is also presented against the classical stochastic optimal control, whereby statistical linearization based LQG is employed to design the optimal controller. It is remarked that the proposed polynomial chaos expansion is a preferred approach to the optimal control of nonlinear random oscillators.

1. Introduction

Classical homogeneous chaos expansion provides a means for representing stochastic processes in terms of multidimensional Hermite polynomials of random variable argument [1,2]. This representation is unique and can be approximated through a sequence of finite order polynomial expansions. The coefficients in these expansions must then be computed in a manner that will ensure suitable convergence (usually in the L^2 sense) to the target random variable or process. A standard procedure for evaluating these coefficients, which guarantees the above convergence, involves orthogonal projections of the error associated either with representing the random function itself or with substituting the polynomial representation of the function into a governing equation [3–5]. This latter approach usually yields a system of equations that govern the behavior of these coupled coefficients. In dynamics problems, these equations are typically evolution equations the solution of which yields the time evolution of the coefficients in these polynomial expansions.

* Corresponding author.
E-mail addresses: pengyongbo@tongji.edu.cn (Y.-B. Peng), ghanem@usc.edu (R. Ghanem), lijie@tongji.edu.cn (J. Li).

0022-460X/$ - see front matter © 2010 Elsevier Ltd. All rights reserved.
doi:10.1016/j.jsv.2010.03.020

The polynomial chaos (PC) expansion thus, when coupled with a Galerkin projection scheme, provides an approximation to the evolution of a dynamical system in the form of an explicit functional dependence on the basic uncertain parameters that characterize the system, and which could relate to the excitation or to system parameters. From these, sample paths of the time-evolving process can be readily synthesized, and estimates of the probability of various events can be computed very efficiently. This functional form provides a convenient characterization of stochastic system dynamics for the design of robust control policies in the presence of uncertainty.

The original implementation of polynomial chaos expansion into problems of mechanics involved Hermite polynomials in Gaussian variables [3–5]. Extensions to other functional forms (other orthogonal polynomials and more general bases) were introduced [6,7] and adapted to various problems in science and engineering. The challenge associated with the length of the expansion, a multidimensional polynomial expansion, was addressed in a number of ways [8,9] ranging from an iterative identification of a parsimonious expansion [8] to an adaptive reconstruction of bases to span the dominant subspace. The work of Li and Ghanem [8] in particular, is well adapted to the topic of the present paper and will be extended herein. In that work, an adaptive polynomial chaos expansion was constructed, which involved identifying key terms through an iterative process. Those terms in a PC representation of the solution process were significant to the characterization of the solution. A modification of that procedure was subsequently introduced [10] where only the cross-product terms in the polynomial expansion were retained thus significantly reducing the computational cost and the efficacy of the algorithm.

Only recently has attention been devoted to the significance of the polynomial chaos decomposition in control problems. Monti et al. [11] first introduced the polynomial chaos theory as a novel approach for the design of the control in a power converter. Hover and Triantafyllou [12] then discussed the application of polynomial chaos in stability and control for a class of second-order nonlinear system, involving the cases of parametric uncertainty, random initial condition and unknown control gain. In some of these early works, due attention was not given to a proper separation of sample path and mean-square properties, which is a paramountly important character of stochastic processes when dealing with control problems. What sets control problems apart in this regard, is the observation and, in general, the parameters of the control law, such as gain, are deterministic quantities, manufactured into the controller. While they can change from one device to the next, their values do not depend on the dynamic state of the system.

The optimal polynomial control, originated from the Hamilton–Jacobi framework, is an efficient procedure for the control of nonlinear systems. The approach was first developed to study a class of nonlinear optimal controls of Duffing oscillators based on series expansions of the optimal cost function and the optimal control function in a Hamilton–Jacobi context [13]. Another class of optimal polynomial controllers implemented in Duffing systems as well, is based upon the Hamilton–Jacobi–Bellman equation and the optimality conditions derived by Bernstein [14], involving the integral of a quadratic cost function plus a special class of polynomial, such that a closed-form analytical solution can be obtained. It is attractive and preferable in that the gain matrices for different parts of the controller can be computed feasibly from the Riccati and Lyapunov equations in case of given appropriate weighting matrices [15].

In the present paper, we investigate the optimal control of a class of Duffing oscillators subjected to random earthquake ground motions by means of polynomial chaos expansions. To that end, we also introduce a novel procedure for reducing and adapting the length of these expansions. The Karhunen–Loeve expansion is employed to represent the random earthquake ground motions, which is detailed in Section 2. Following that, the proposed adaptation scheme for polynomial chaos construction is described and compared with previous adaptive refinements of stochastic approximation in Section 3. Then, the procedure and numerical cases of stochastic optimal polynomial control of Duffing systems is elucidated in Sections 4 and 5, using the polynomial chaos expansions and the parameters of control policy based on Lyapunov asymptotic stability condition. In order to validate this stochastic optimal control strategy, an investigation is carried out which involves a Linear Quadratic Gaussian (LQG) control obtained through a statistical linearization of the dynamics. In this case, the band-limited white noise input, describing the ground motion, is estimated from the same (simulated) earthquake database so as to synthesize the colored noise used in the proposed algorithm, thus providing legitimacy to the comparison of the two controllers. The concluding remarks are included in Section 6.

2. Discrete representation of seismic processes

A stochastic ground motion model with peak acceleration 0.3g is employed in the following investigation, which is represented by the Karhunen–Loeve (KL) expansion:

$$\ddot{x}_g(\boldsymbol{\Theta},t) = \sum_{i=0}^{\infty} \sqrt{\lambda_i}\ddot{x}_{g,i}(t)\xi_i, \tag{1}$$

where $\{\xi_i\}$ forms a vector of uncorrelated, zero-mean random variables with unit variance. The coefficients λ_i and the functions $\ddot{x}_{g,i}(t)$ are obtained as the solution to the following integral eigenvalue problem:

$$\int_0^T R_{\ddot{x}_g\ddot{x}_g}(t,s)\ddot{x}_{g,i}(s)\,\mathrm{d}s = \lambda_i\ddot{x}_{g,i}(t), \tag{2}$$

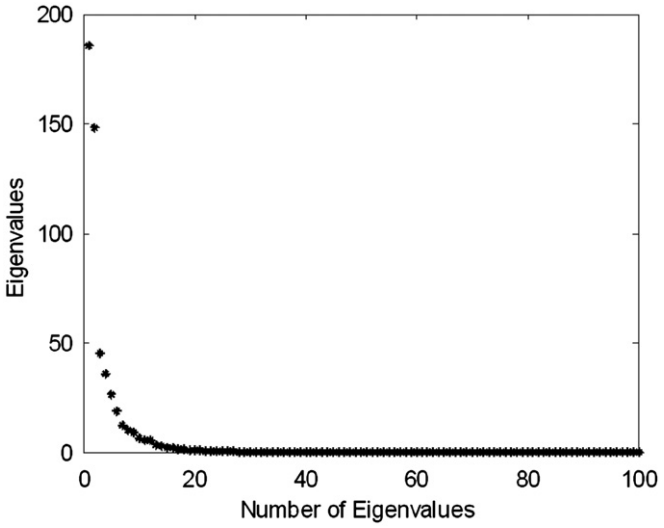

Fig. 1. Discrete representation of seismic processes: the former 100 eigenvalues of the correlation matrix.

where $R_{\ddot{x}_g\ddot{x}_g}(t,s)$ denotes the correlation function of the process $\ddot{x}_g(\boldsymbol{\Theta},t)$ over the time interval [0 T], which is synthesized through statistical averaging from a database of simulated non-stationary seismic processes [16]. In the above, the argument $\boldsymbol{\Theta}$ represents random parameters, such as local site effects, on which the ground depends. These parameters are generally dependent and correlated. Furthermore, the process $\ddot{x}_g(\boldsymbol{\Theta},t)$ depends on them in some complicated nonlinear manner. The KL expansion transforms this functional dependence on the set $\boldsymbol{\Theta}$ into a linear dependence on a set $\{\xi_i\}$, consisting of uncorrelated random variables. For Gaussian processes, as will be assumed in this paper, these random variables form an independent Gaussian vector, otherwise they are determined by their joint density function which can be estimated from experimental measurements on the process $\ddot{x}_g(\boldsymbol{\Theta},t)$ [17]. It is noted that the rate of decay of the magnitude of eigenvalues of the integral equation depends on the correlation length of the random process, the longer the correlation length, the fewer terms being required in the expansion in order to achieve a comparable accuracy. Fig. 1 shows the magnitude of its first 100 eigenvalues, indicating that 99 percent of the variance is carried by the first 24 eigenvalues.

As indicated in the introduction, an LQG controller is implemented for comparison purposes. In this case, a band-limited white noise is used to describe the ground motion. To justify the comparison between the two controllers, the strength of this signal is designed so as to be compatible with the same database from which the above correlation function is computed.

3. Updated scheme of adaptive polynomial chaos

We consider a hardening Duffing oscillator subjected to random earthquake ground motion, governed by the following equation:

$$\ddot{x}(t)+2\zeta\omega_0\dot{x}(t)+\omega_0^2[x(t)+\mu x^3(t)]=-\ddot{x}_g(\boldsymbol{\Theta},t),\quad x(t_0)=\dot{x}(t_0)=0. \tag{3}$$

where $x(t)$ is the oscillator displacement, μ represents the nonlinearity level of the oscillator, the damping ratio ζ and the natural frequency ω_0 are assumed to be 0.02 and 2 rad/s, respectively. The stochastic ground motion model $\ddot{x}_g(\boldsymbol{\Theta},t)$ is represented by a Karhunen–Loeve expansion truncated at the M^{th} term and the solution to Eq. (3) is sought as a truncated polynomial chaos expansion in the form:

$$x(t)=\sum_{i=0}^{P} x_i(t)\boldsymbol{\Psi}_i(\boldsymbol{\xi}), \tag{4}$$

where $\boldsymbol{\xi}$ denotes an M-dimensional Gaussian vector $\{\xi_i\}_{i=1}^{M}$, and P is the number of terms retained in the expansion; $x_i(t)$ are unknown deterministic functions while $\{\boldsymbol{\Psi}_i(\boldsymbol{\xi})\}$ denote the polynomial chaoses, which are Hermite polynomials in the random variables $\{\xi_i\}$. It is noted that the statistics of the response can be computed and the probability density function for quantities of interest can be estimated via numerical quadrature or Monte Carlo simulation once $x_i(t)$ have been evaluated. Expanding the right-hand side of Eq. (3) in its Karhunen–Loeve series Eq. (1), and introducing the polynomial chaos expansion Eq. (4), the equation of motion becomes,

$$\sum_{i=0}^{P}[\boldsymbol{\Psi}_i(\boldsymbol{\xi})(\ddot{x}_i(t)+2\zeta\omega_0\dot{x}_i(t)+\omega_0^2x_i(t))]+\omega_0^2\mu\sum_{i=0}^{P}\sum_{j=0}^{P}\sum_{k=0}^{P}\boldsymbol{\Psi}_i(\boldsymbol{\xi})\boldsymbol{\Psi}_j(\boldsymbol{\xi})\boldsymbol{\Psi}_k(\boldsymbol{\xi})x_i(t)x_j(t)x_k(t)=-\sum_{i=0}^{M}\sqrt{\lambda_i}\ddot{x}_{g,i}(t)\xi_i. \tag{5}$$

The above equation is projected onto the random space spanned by the orthogonal polynomial basis $\Psi_m(\xi)$, i.e., taking the inner product with each basis and then using their orthogonality relation, yields a set of coupled deterministic nonlinear differential equations:

$$\ddot{x}_m(t)+2\zeta\omega_0\dot{x}_m(t)+\omega_0^2 x_m(t)=-\frac{\omega_0^2\mu}{\langle\Psi_m^2\rangle}\sum_{i=0}^{M}\sum_{j=0}^{M}\sum_{k=0}^{M}c_{ijkm}x_i(t)x_j(t)x_k(t)-\sqrt{\lambda_m}\ddot{x}_{g,m}(t), \tag{6}$$

where $x_m(0)=\dot{x}_m(0)=0$, m=0,1,2,…,P, $c_{ijkm}=\langle\Psi_i\Psi_j\Psi_k\Psi_m\rangle$, and $\sqrt{\lambda_m}\ddot{x}_{g,m}(t)$ vanishes for $m>M$; here $\langle\cdot\rangle$ denotes an ensemble average. The coefficients c_{ijkm} and $\langle\Psi_m^2\rangle$ can be determined analytically or numerically using multidimensional numerical quadratures. The system of equations consists of (P+1) nonlinear deterministic equations with each equation corresponding to one PC mode, which could be readily solved using standard techniques for deterministic differential equations. An adaptive step-size fourth-order Runge–Kutta routine is employed to solve these nonlinear differential equations.

The number of (P+1) terms required in the expansion grows very rapidly as the number of terms (M+1) in the expansion for the seismic process $\ddot{x}_g(\Theta,t)$ and the order p in the polynomial chaoses $\{\Psi_i(\xi)\}$ increases. However, not all the terms in the expansion for $x(t)$ contribute significantly to the sum. An adaptive scheme, first presented by Li and Ghanem [8], was designed to retain only a K-dimensional subset of the M random variables ξ_i which is responsible for most of the fluctuations in the solution process. A displacement–energy criterion was used in determining the magnitude of these contributions [8]. The expansion of the solution is then written as

$$x(t)=\overline{x}(t)+\sum_{i=1}^{K}x_i(t)\Psi_i(\xi)+\sum_{i=K+1}^{M}x_i(t)\Psi_i(\xi)+\sum_{j=M+1}^{N}x_j(t)\Psi_j(\xi_i|_{i=1}^{K}),\quad N\le P, \tag{7}$$

where N is the highest term of the adaptive polynomial chaos expansion. It is noted that the first two summations represent the linear contributions, while the third summation involves higher-order terms in the forms of polynomials with the random variables only included in the first summation, and the higher-order contributions of the terms contained in the second summation will be neglected. The displacement–energy in the criterion is represented by the norm of each PC mode $x_i(t)$ over the time interval:

$$\|x_i(t)\|=\sum_{j=1}^{N_T}x_i^2(t_j)\Delta t_j,\quad i=0,\ldots,M, \tag{8}$$

where N_T denotes the number of time steps used in numerical integration. The K linear components $x_i(t)$, among $i\le M$ with the largest norm, are sorted and recorded, and then used to generate the higher-order components in the next iteration. The iterative process is repeated until the ordering of the K largest contributors to the solution does not change.

Another extended adaptive procedure, keeping only the nonlinear terms corresponding to cross products between random dimensions, was proposed as a refinement of the above procedure, and justified by the observation of dominant modal energy of these cross-terms [10]. The coefficients corresponding to the nonlinear polynomials of the form:

$$\Psi_j(\xi_i|_{i=1}^{K})=\prod\boldsymbol{C}_l^{\xi_1,\ldots,\xi_i,\ldots,\xi_K},\quad l=1,2,\ldots,K, \tag{9}$$

where the operator $\prod\boldsymbol{C}_l^{\xi_1,\ldots,\xi_i,\ldots,\xi_K}$ represents the product of the combination of the K possible linear polynomials in ξ_i taken l at a time. It is noted that this modified adaptive procedure does not modify the ordering criterion based on displacement energy. The validity of this modification, moreover, is specific to certain special cases, as shown below in one of the examples. Recalling that the trajectory of the oscillator depends on both its displacement and velocity, a revised ordering criterion is proposed as follows:

$$\|y_i(t)\|=\|x_i(t)\|+\|\dot{x}_i(t)\|=\sum_{j=1}^{N_T}x_i^2(t_j)\Delta t_j+\sum_{j=1}^{N_T}\dot{x}_i^2(t_j)\Delta t_j,\quad i=0,\ldots,M. \tag{10}$$

Fig. 2 depicts the largest contributors of a cubic-order adaptive polynomial chaos employed in the analysis of a nonlinear random oscillator ($K=4$,$M=24$,$N=54$,$p=3$,$\mu=200$), using both the displacement criterion given by Eq. (8) and the displacement–velocity criterion given by Eq. (10), respectively. It is noted that the two criteria feature distinctively different ordering of the K largest contributors over the time interval to the solution process. Thus, whereas the first two largest contributors for each of the two criterions are identified with the first and second random variables, the third and fourth largest contributors vary with time, with the variations being more pronounced and of higher frequency using a displacement-only criterion. The effect of this re-ordering on the predicted evolution of the solution process is next examined.

In order to investigate the proposed adaptation scheme for the polynomial chaos expansion, the second-order statistics of five illustrative cases of a nonlinear random oscillator with nonlinearity level $\mu=200$ are examined. Case 1, labelled PC-I, shows the solution using polynomial chaos decomposition with parameters: (K=24, M=24, N=24, p=1); Case 2, labelled PC-II, corresponds to the parameters set: (K=4, M=4, N=34, p=3); Case 3, labelled APC-I, corresponds to an adaptive polynomial chaos expansion with displacement criterion and parameters: (K=4, M=24, N=54, p=3); Case 4, labelled APC-II, is associated with an adaptive expansion with velocity and displacement criterion and parameters: (K=4,

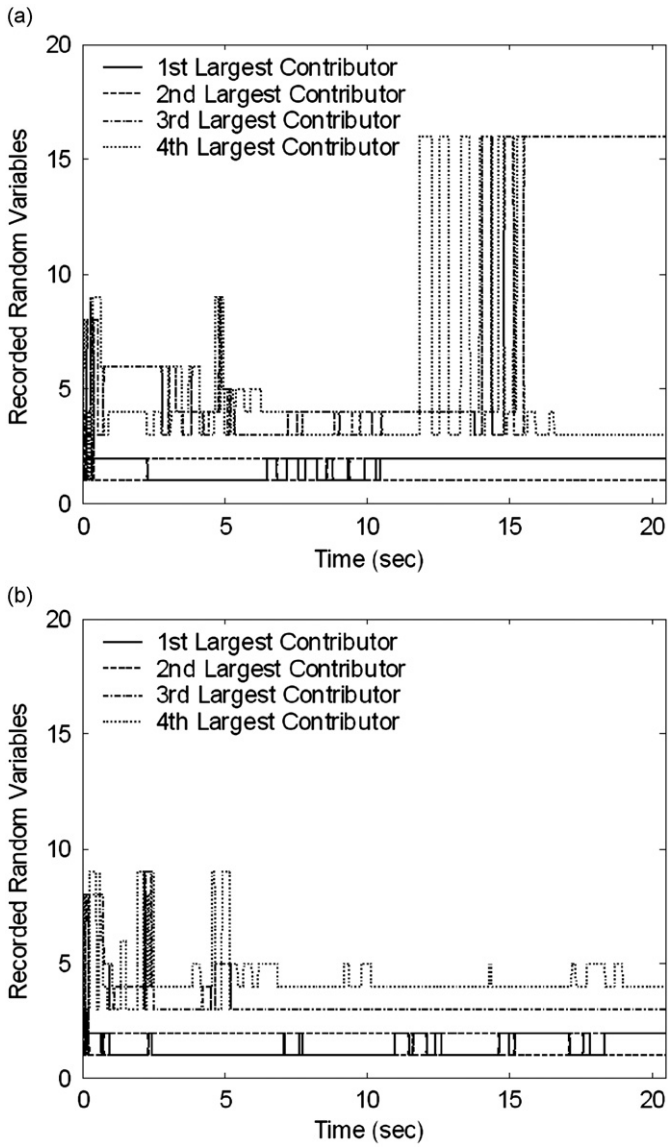

Fig. 2. Updated scheme of adaptive polynomial chaos: the four largest contributors of adaptive polynomial chaos as two different criteria: (a) displacement criterion and (b) displacement–velocity criterion ($K=4, M=24, N=54, p=3, \mu=200$).

M=24, N=54, p=3); Finally, Case 5, labelled MC, corresponds to a Monte Carlo simulation solution with parameters: (M=24, 10,000 events). As shown in Fig. 3, the solutions of the two adaptive schemes (Cases 3 and 4) approach the Monte Carlo solution more closely than the other two cases, indicating that the adaptive schemes are indeed suitable for reducing the dimensionality of the expansion while maintaining accuracy. The numerical results from Case 1 appear to be superior to those of Case 2, and closer to the adaptive polynomial chaos solutions, indicating that the number of random variables used in the polynomial chaos expansion is reasonably sufficient for capturing the essential system dynamics. There is also an indication that including a sufficient number of random variables in the polynomial chaos expansion is more important than carrying out the expansion to a higher order.

It is recognized that the first two random variables carry most of the fluctuations of the response since the solutions of two the adaptive schemes are almost identical over the entire time domain, and the difference between them lies mainly in the allocation of contributions from terms beyond the third random variable. An L_2 error norm comparison between the adaptive schemes and Monte Carlo solution details their differences. The error on root-mean-square displacements between the adaptive polynomial chaos APC-I and Monte Carlo solution is 0.1286, and the error on root-mean-square velocities between them is 0.2208; while the error on root-mean-square displacements between the adaptive polynomial chaos APC-II and Monte Carlo solution is 0.1284, the error of their root-mean-square velocities being 0.2200. It reveals that

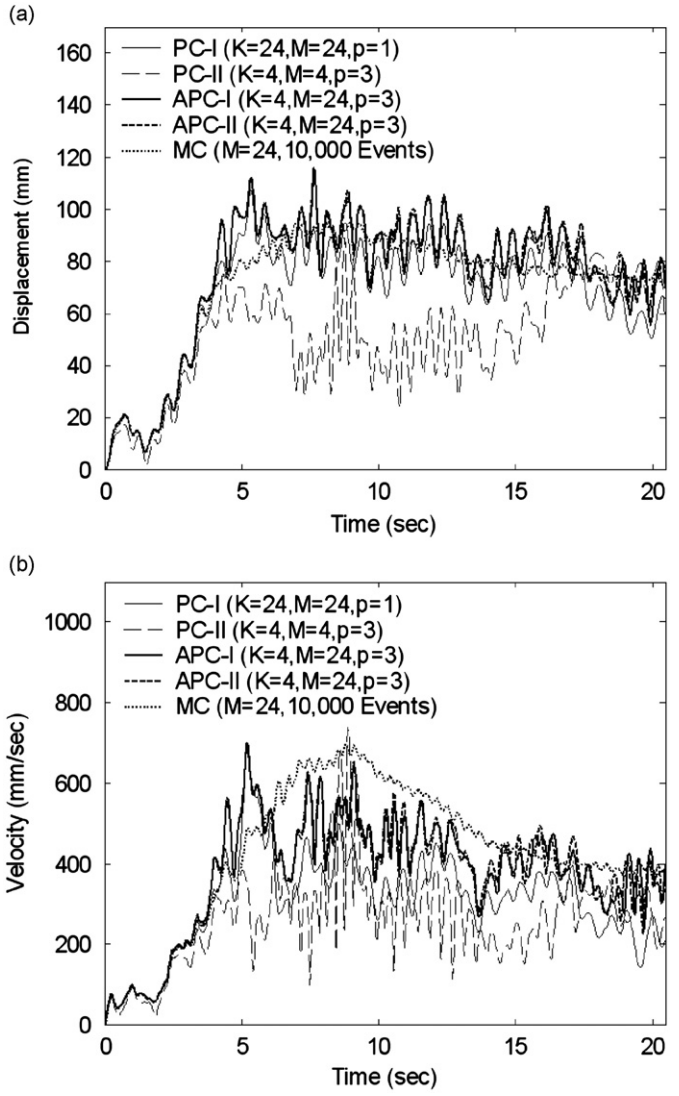

Fig. 3. Updated scheme of adaptive polynomial chaos: comparison between second-order statistics of responses obtained by polynomial chaos expansions and those by Monte Carlo simulation about (a) root-mean-square relative displacement and (b) root-mean-square relative velocity ($\mu = 200$).

the updated adaptive polynomial chaos using the displacement–velocity criterion is slightly superior to the adaptive polynomial chaos using the displacement criterion.

4. Polynomial chaos expansions on optimal polynomial controller

When a base-excited Duffing oscillator is subjected to a control force, the equation of motion becomes,

$$\ddot{x}(t)+2\zeta\omega_0\dot{x}(t)+\omega_0^2[x(t)+\mu x^3(t)] = u(t)-\ddot{x}_g(\boldsymbol{\Theta},t), \quad x(t_0)=\dot{x}(t_0)=0, \tag{11}$$

where $u(t)$ is a scaled control force per unit mass. In the state space form, Eq. (11) can be written as

$$\dot{\mathbf{Z}}(t) = \boldsymbol{\Lambda}(\mathbf{Z})\mathbf{Z}(t)+\mathbf{B}u(t)+\mathbf{D}\ddot{x}_g(\boldsymbol{\Theta},t), \tag{12}$$

with the initial state $\mathbf{Z}(t_0)=\boldsymbol{z}_0$, where $\mathbf{Z}(t)$ is a 2-dimensional state vector; $\boldsymbol{\Lambda}(\mathbf{Z})$ is a (2×2) gradient matrix; $\mathbf{B}$ is (2×1) controller location matrix; $\mathbf{D}$ is (2×1) base-excitation location matrix, respectively,

$$\mathbf{Z}(t)=\begin{bmatrix} x(t) \\ \dot{x}(t) \end{bmatrix}, \quad \boldsymbol{\Lambda}(\mathbf{Z})=\begin{bmatrix} 0 & 1 \\ -(1+\mu x^2(t))\omega_0^2 & -2\zeta\omega_0 \end{bmatrix}, \quad \mathbf{B}=\begin{bmatrix} 0 \\ 1 \end{bmatrix}, \quad \mathbf{D}=\begin{bmatrix} 0 \\ -1 \end{bmatrix}. \tag{13}$$

There exists two points of view regarding the investigation of the motion of physical stochastic systems [18]. One is the state space description (also called Eulerian description) underling classical stochastic optimal control, whereby the system is modeled using an Ito stochastic differential equation driven by white noise or filtered white noise. The corresponding response process exhibits a Markov property, the transition probability for which is governed by the Foker–Planck–Kolmogorov equation. The other refers to random event description (namely Lagrangian description), where the system is represented by stochastic differential equation with random excitation term not subject to the white noise assumption, and the corresponding transition probability of response process satisfies the generalized density evolution equation. The latter point promotes a physical approach to structural stochastic optimal controls [19]. Here, we advocate the random event description of physical stochastic systems due to the essential non-white property of external excitations driving on nonlinear random oscillators in practical engineering.

For a given realization $\boldsymbol{\theta}$ of the stochastic parameter vector $\boldsymbol{\Theta}$, a polynomial cost function is given by

$$J(\mathbf{Z},u,\boldsymbol{\theta},t)=\mathbf{S}(\mathbf{Z}(t_f),t_f)+\frac{1}{2}\int_{t_0}^{t_f}[\mathbf{Z}^{\mathrm{T}}(t)\mathbf{Q}\mathbf{Z}(t)+\mathbf{R}u^2(t)+\boldsymbol{h}(\mathbf{Z},t)]\,\mathrm{d}t, \tag{14}$$

where $\mathbf{S}(\mathbf{Z}(t_f),t_f)$ is the terminal cost; t_0,t_f are the start time and terminal time, respectively, $\mathbf{Q}$ is a (2×2) positive semi-definite state weighting matrix; $\mathbf{R}$ is a (1×1) positive-definite control weighting matrix; $\boldsymbol{h}(\mathbf{Z},t)$ is the higher-order term of the cost function with orders being higher than quadratic. The minimization of the cost Eq. (14) results in the Hamilton–Jacobi–Bellman equation [20]:

$$\frac{\partial V}{\partial t}=-\min_u[H(\mathbf{Z},u,V'(\mathbf{Z},t),t)], \tag{15}$$

where a prime indicates differentiation with respect to $\mathbf{Z}$; $V(\mathbf{Z},t)$ is the optimal cost function, satisfying all the properties of a Lyapunov function [14], considered as

$$V(\mathbf{Z},t)=\tfrac{1}{2}\mathbf{Z}^{\mathrm{T}}(t)\mathbf{P}(t)\mathbf{Z}(t)+g(\mathbf{Z},t), \tag{16}$$

where $\mathbf{P}(t)$ is a (2×2) Riccati matrix, and $g(\mathbf{Z},t)$ is a positive definite multinomial in $\mathbf{Z}(t)$ that is chosen in the following form [21]:

$$g(\mathbf{Z},t)=\sum_{i=2}^{k}\frac{1}{i}[\mathbf{Z}^{\mathrm{T}}(t)\mathbf{M}_i(t)\mathbf{Z}(t)]^i, \tag{17}$$

where $\mathbf{M}_i(t), i=2,3,\ldots,k$ are Lyapunov matrices to be defined later.

Since initial state $\mathbf{Z}(t_0)=\mathbf{0}$ is the stable equilibrium point to the oscillator system in a broad sense, the external excitation $\ddot{x}_g(\boldsymbol{\Theta},t)$ does not affect the system stability, and can be neglected in deriving the controller. The Hamiltonian function $H(\cdot)$ is given by

$$H(\mathbf{Z},u,V'(\mathbf{Z},t),t)=\tfrac{1}{2}[\mathbf{Z}^{\mathrm{T}}(t)\mathbf{Q}\mathbf{Z}(t)+\mathbf{R}u^2(t)+\boldsymbol{h}(\mathbf{Z},t)]+[V'(\mathbf{Z},t)]^{\mathrm{T}}(\boldsymbol{\Lambda}\mathbf{Z}(t)+\mathbf{B}u(t)), \tag{18}$$

where $\boldsymbol{h}(\mathbf{Z},t)$ is defined as the following function of $g(\mathbf{Z},t)$, so as to construct the solution $\mathbf{P}(t)$ of Riccati matrix equation and the solution $\mathbf{M}_i(t)$ of Lyapunov matrix:

$$\boldsymbol{h}(\mathbf{Z},t)=2\sum_{i=2}^{k}[\mathbf{Z}^{\mathrm{T}}(t)\mathbf{M}_i\mathbf{Z}(t)]^{i-1}\mathbf{Z}^{\mathrm{T}}(t)\mathbf{Q}_i\mathbf{Z}(t)+4\left[\sum_{i=2}^{k}[\mathbf{Z}^{T}(t)\mathbf{M}_i\mathbf{Z}(t)]^{i-1}\mathbf{M}_i\mathbf{Z}(t)\right]^{\mathrm{T}}\mathbf{B}\mathbf{R}^{-1}\mathbf{B}^{\mathrm{T}}\left[\sum_{i=2}^{k}[\mathbf{Z}^{T}(t)\mathbf{M}_i\mathbf{Z}(t)]^{i-1}\mathbf{M}_i\mathbf{Z}(t)\right]. \tag{19}$$

One could realize that $\mathbf{P}(t)$ and $\mathbf{M}_i(t)$ are both related with the gradient matrix $\boldsymbol{\Lambda}(\mathbf{Z})$, indicating that the control gain of the polynomial controller $u(t)$ cannot be calculated off-line. An approximate solution to the control gain is obtained by linearizing $\boldsymbol{\Lambda}(\mathbf{Z})$ at the initial equilibrium point $\mathbf{Z}=\mathbf{0}$ [21], i.e., replacing $\boldsymbol{\Lambda}(\mathbf{Z})$ in Eq. (18) by $\boldsymbol{\Lambda}_0$, $\boldsymbol{\Lambda}_0=\boldsymbol{\Lambda}(\mathbf{Z})|_{\mathbf{Z}=\mathbf{0}}$. Hence, an optimal polynomial controller is obtained analytically in the form:

$$u(t)=-\mathbf{R}^{-1}\mathbf{B}^{\mathrm{T}}\mathbf{P}(t)\mathbf{Z}(t)-\mathbf{R}^{-1}\mathbf{B}^{\mathrm{T}}\sum_{i=2}^{k}[\mathbf{Z}^{T}(t)\mathbf{M}_i(t)\mathbf{Z}(t)]^{i-1}\mathbf{M}_i(t)\mathbf{Z}(t), \tag{20}$$

where $\mathbf{P}(t)$ and $\mathbf{M}_i(t)$ could be further approximately evaluated as constant matrices $\mathbf{P},\mathbf{M}_i$ by solving the following algebraic Riccati and Lyapunov equations, i.e. the steady-state Riccati and Lyapunov matrix equations, respectively

$$\mathbf{P}\boldsymbol{\Lambda}_0+\boldsymbol{\Lambda}_0^{\mathrm{T}}\mathbf{P}-\mathbf{P}\mathbf{B}\mathbf{R}^{-1}\mathbf{B}^{\mathrm{T}}\mathbf{P}+\mathbf{Q}=\mathbf{0}, \tag{21}$$

$$\mathbf{M}_i(\boldsymbol{\Lambda}_0-\mathbf{B}\mathbf{R}^{-1}\mathbf{B}^{\mathrm{T}}\mathbf{P})+(\boldsymbol{\Lambda}_0-\mathbf{B}\mathbf{R}^{-1}\mathbf{B}^{\mathrm{T}}\mathbf{P})^{\mathrm{T}}\mathbf{M}_i+\mathbf{Q}_i=\mathbf{0},\quad i=2,3,\ldots,k. \tag{22}$$

Eqs. (21) and (22) can be solved using any well-known numerical algorithms or using toolbox functions available in MATLAB, and the state-feedback controller becomes,

$$u(t)=-\mathbf{R}^{-1}\mathbf{B}^{\mathrm{T}}\mathbf{P}\mathbf{Z}(t)-\mathbf{R}^{-1}\mathbf{B}^{\mathrm{T}}\sum_{i=2}^{k}[\mathbf{Z}^{\mathrm{T}}(t)\mathbf{M}_i\mathbf{Z}(t)]^{i-1}\mathbf{M}_i\mathbf{Z}(t). \tag{23}$$

The optimal polynomial controller in Eq. (23) consists of linear and nonlinear terms. The linear term with the first-order polynomial is the same as that of the linear quadratic regulator (LQR), while the nonlinear term of the controller consists of odd-order multinomials hinging on the states of the system, e.g. cubic, quintic etc. The polynomial chaos expansion of the polynomial controller is given by

$$\sum_{j=0}^{P} u_j(t)\Psi_j(\xi) = -\mathbf{R}^{-1}\mathbf{B}^{\mathrm{T}}\mathbf{P}\sum_{j=0}^{P}\mathbf{Z}_j(t)\Psi_j(\xi) - \mathbf{R}^{-1}\mathbf{B}^{\mathrm{T}}\sum_{i=2}^{k}\left[\sum_{r_i=0}^{P}\mathbf{Z}_{r_i}^{\mathrm{T}}(t)\Psi_{r_i}(\xi)\mathbf{M}_i\sum_{s_i=0}^{P}\mathbf{Z}_{s_i}(t)\Psi_{s_i}(\xi)\right]^{i-1}\mathbf{M}_i\sum_{j=0}^{P}\mathbf{Z}_j(t)\Psi_j(\xi), \tag{24}$$

where $\mathbf{Z}_j(t) = [x_j(t)\ \dot{x}_j(t)]^{\mathrm{T}}$. The solution of Eq. (24) obtained through Galerkin projection is given as

$$u_m(t) = -\mathbf{R}^{-1}\mathbf{B}^{\mathrm{T}}\mathbf{P}(t)\mathbf{Z}_m(t) - \mathbf{R}^{-1}\mathbf{B}^{\mathrm{T}}\sum_{i=2}^{k}\sum_{r_2=0}^{P}\cdots\sum_{r_i=0}^{P}\sum_{s_2=0}^{P}\cdots\sum_{s_i=0}^{P}\sum_{j=0}^{P}\frac{\langle\Psi_{r_2}\cdots\Psi_{r_i}\Psi_{s_2}\cdots\Psi_{s_i}\Psi_j\Psi_m\rangle}{\langle\Psi_m^2\rangle}[\mathbf{Z}_{r_i}^{\mathrm{T}}(t)\mathbf{M}_i\mathbf{Z}_{s_i}(t)]^{i-1}\mathbf{M}_i\mathbf{Z}_j(t). \tag{25}$$

Since the linear term has the most significant contribution to the controller, an approximate form for the control force, neglecting the cross-terms in Eq. (25), is given by

$$u_m(t) = -\mathbf{R}^{-1}\mathbf{B}^{\mathrm{T}}\mathbf{P}(t)\mathbf{Z}_m(t) - \mathbf{R}^{-1}\mathbf{B}^{\mathrm{T}}\sum_{i=2}^{k}\frac{\langle\Psi_m^i\rangle}{\langle\Psi_m^2\rangle}[\mathbf{Z}_m^{\mathrm{T}}(t)\mathbf{M}_i\mathbf{Z}_m(t)]^{i-1}\mathbf{M}_i\mathbf{Z}_m(t). \tag{26}$$

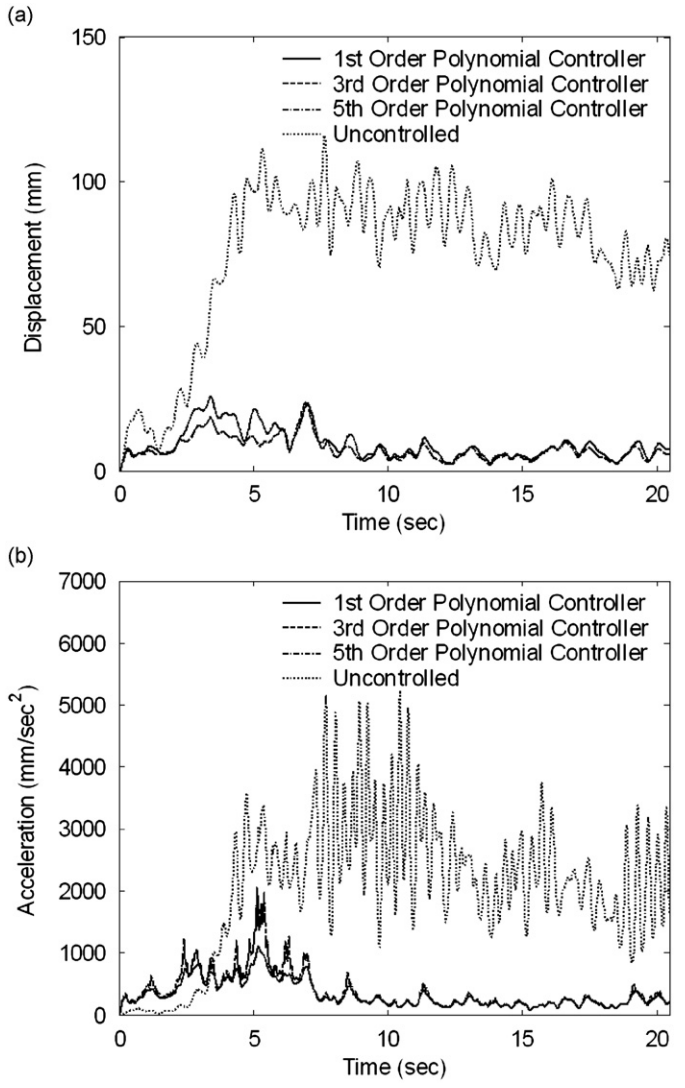

Fig. 4. Optimal polynomial control of nonlinear random oscillators: time histories of root-mean-square responses of Duffing oscillator with/without control: (a) relative displacement and (b) absolute acceleration (APC-II, $\mu = 200$).

then, the controller is synthesized by the following polynomial chaos expansion:

$$u(t) = \sum_{j=0}^{P} u_j(t)\Psi_j(\xi), \tag{27}$$

from which statistics and probability density function of the optimal control force can be calculated.

5. Optimal polynomial control of nonlinear random oscillators

It is noted that the preceding controlled nonlinear oscillators are considered as completely observed systems, i.e. the states of the systems are assumed to be known exactly, and the resulting nonlinear controller, represented by Eq. (23), is designed for a specific sample from the set of random event. The presence of randomness in system parameters raises the question as to the meaning of optimality for these systems. The current approach, addresses that question in the following manner: for each element θ of the sample space, a control force is computed. A parameterization of $u(t)$ as a function of θ is then constructed in the form of the polynomial chaos expansion, and thought of as a description of the functional dependence of the control force on the uncertain parameters $\boldsymbol{\Theta}$. Although not carried out in the present paper, this stochastic description of the control force permits additional constraints to be accommodated in the control design. Specifically, the matrices $\mathbf{Q}$ and $\mathbf{R}$ can be so selected as to minimize some additional probabilistic measure of the system dynamics. The classical stochastic optimal control is to seek the control force in an admissible set by minimizing or maximizing the cost function in the mean-square sense of system states [22,23], and the control gain appears as a deterministic function in gain parameters spontaneously. A fair amount of research on this subject, in the context of

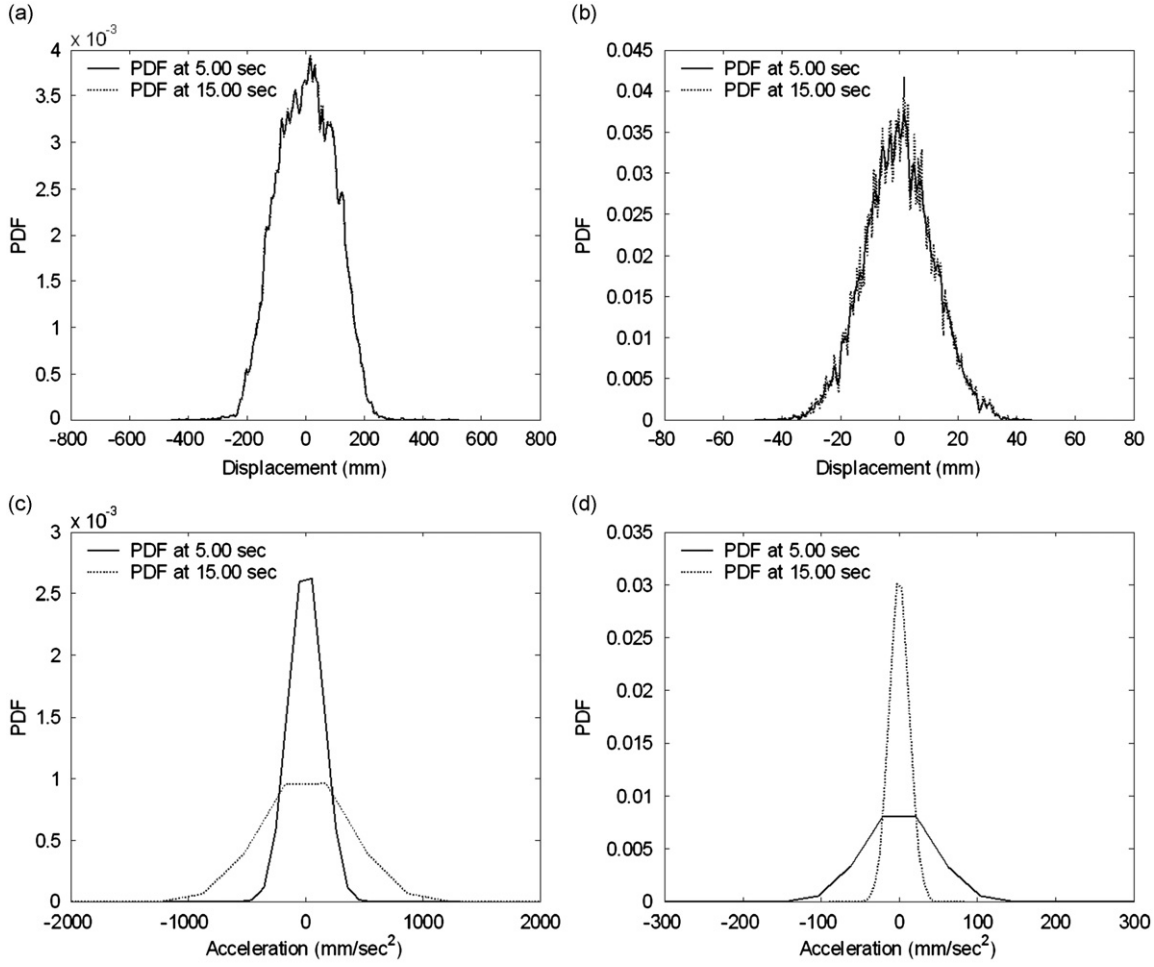

Fig. 5. Optimal polynomial control of nonlinear random oscillators: PDFs of responses of Duffing oscillator at typical moments with/without control: (a) uncontrolled relative displacement, (b) controlled relative displacement, (c) uncontrolled absolute acceleration and (d) controlled absolute acceleration (APC-II, $\mu = 200$). Uncontrolled relative displacement.

classical stochastic optimal control, has been devoted in recent years, e.g., probabilistically-optimal control of system robustness [24]; reliability-based optimal structural control [25,26]; optimal feedback control for quasi-Hamiltonian systems [27]; covariance controller with specified reliability level [28]; and covariance control tracking pre-specified probability density functions (PDFs) [29]. In the following numerical investigation, the control gain is obtained by defining the weighting matrices based on the Lyapunov asymptotic stability condition of systems [30]: $\mathbf{Q}=\mathrm{diag}\{80.0,20.0\}$, $\mathbf{R}=1.0$, $\mathbf{Q}_2=\mathrm{diag}\{50.0,15.0\}$, $\mathbf{Q}_i=\mathrm{diag}\{20.0,5.0\}$, i=3,4,….

Time histories of root-mean-square responses including the relative displacement and absolute acceleration of a Duffing oscillator ($\mu=200$) with and without polynomial controllers are pictured in Fig. 4. It is observed that system displacement and acceleration are reduced greatly with polynomial controllers designed by the updated adaptive scheme (APC-II). It is noted that the effects of the controllers with different orders are almost identical, and the higher-order controllers have better displacement controlled than that of the first-order controller, while have worse acceleration controlled. One could see that the third-order controller reaches a close control effect to the fifth-order controller, indicating that the third-order controller is definitely satisfactory to the investigated Duffing oscillator if the displacement related to system safety is of principle concern. A third-order controller is thus employed in ascertaining the performance of the control algorithm. Fig. 5 shows the PDFs of the relative displacement and absolute acceleration of the controlled and uncontrolled Duffing oscillator at time instants 5 and 15 s. It is clear that the distribution domain of the controlled PDFs all

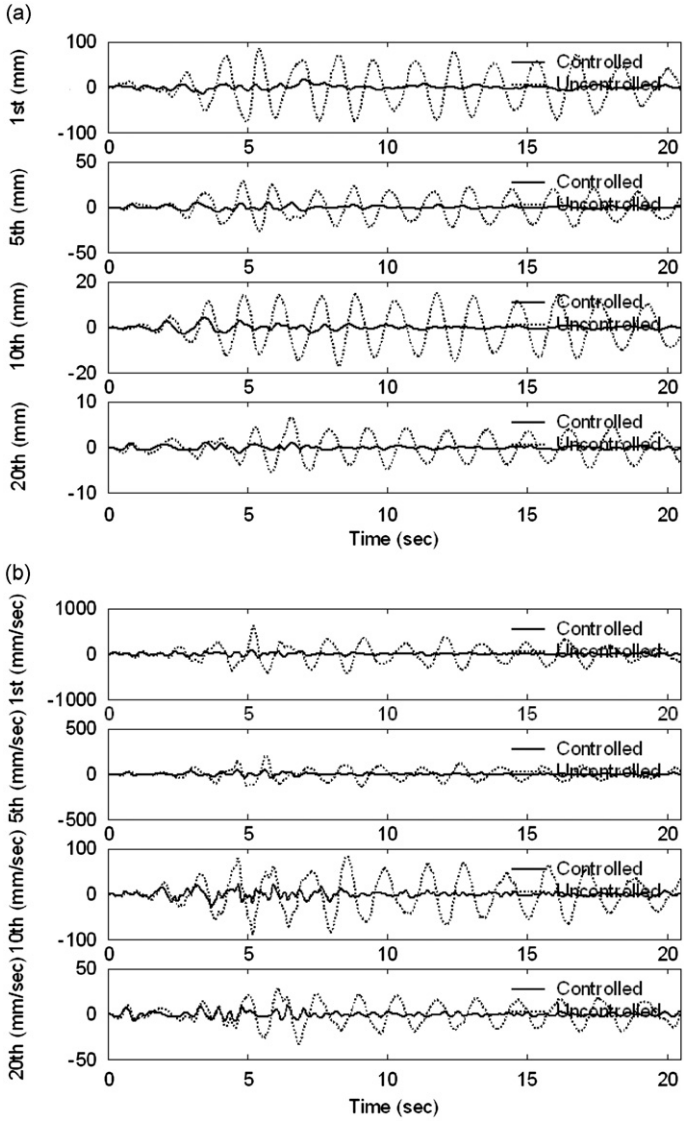

Fig. 6. Optimal polynomial control of nonlinear random oscillators: typical PC modes of polynomial chaos expansion with/without control: (a) displacement modes and (b) velocity modes (APC-II, $\mu=200$).

become much smaller, nearly one tenth of the distribution domain of the uncontrolled ones, which is consistent with changes of magnitudes of the root-mean-square responses shown in Figs. 4(a) and (b). Moreover, the PDFs of the uncontrolled responses at two typical times approximately admit Gaussian distributions. The PDFs of the controlled responses, however, nearly admit Gaussian distributions, indicating that the nonlinear level of the system degrades after controlled.

Fig. 6 shows the time evolutions of typical PC modes of polynomial chaos expansion with and without control. It is noted that the contributions of PC modes, whether to the relative displacement or to the relative velocity, are greatly reduced in the controlled system, indicating that the length of a sufficient polynomial chaos expansion can itself be reduced. It is also noted that the reduction in the typical PC modes is almost the same for all PC modes. A further investigation on the performance of PC modes addresses their phase plane evolution, as depicted in Fig. 7. It is seen that the uncontrolled orbits of the two typical PC modes begin with stable closed orbits at the innermost layer, then jump to outer layers and moving around there. This kind of jump phenomenon is the well-known bifurcations; see Figs. 7(a) and (c). However, the controlled orbits of the modes, pictured in Figs. 7(b) and (d), basically move around the equilibrium points, revealing that the bifurcations become more active in the presence of the stochastic optimal control.

Fig. 8 shows the norm distribution of the PC modes, including displacement modes and velocity modes, of the polynomial chaos expansion with and without control. Four regions are marked according to the orders of homogenous chaos to outline the essential contributors. The regions $p=0$, $p=1$, $p=2$, $p=3$ in the figure represent the modes associated with constant terms, linear terms, quadratic terms and cubic terms of polynomials, respectively. It is clear, as expected, that the modes associated with $p=0$ and $p=2$ are zero. This is true in that the represented random earthquake ground motion possesses zero-mean, and only the PC modes associated with polynomials of odd orders are excited due to the

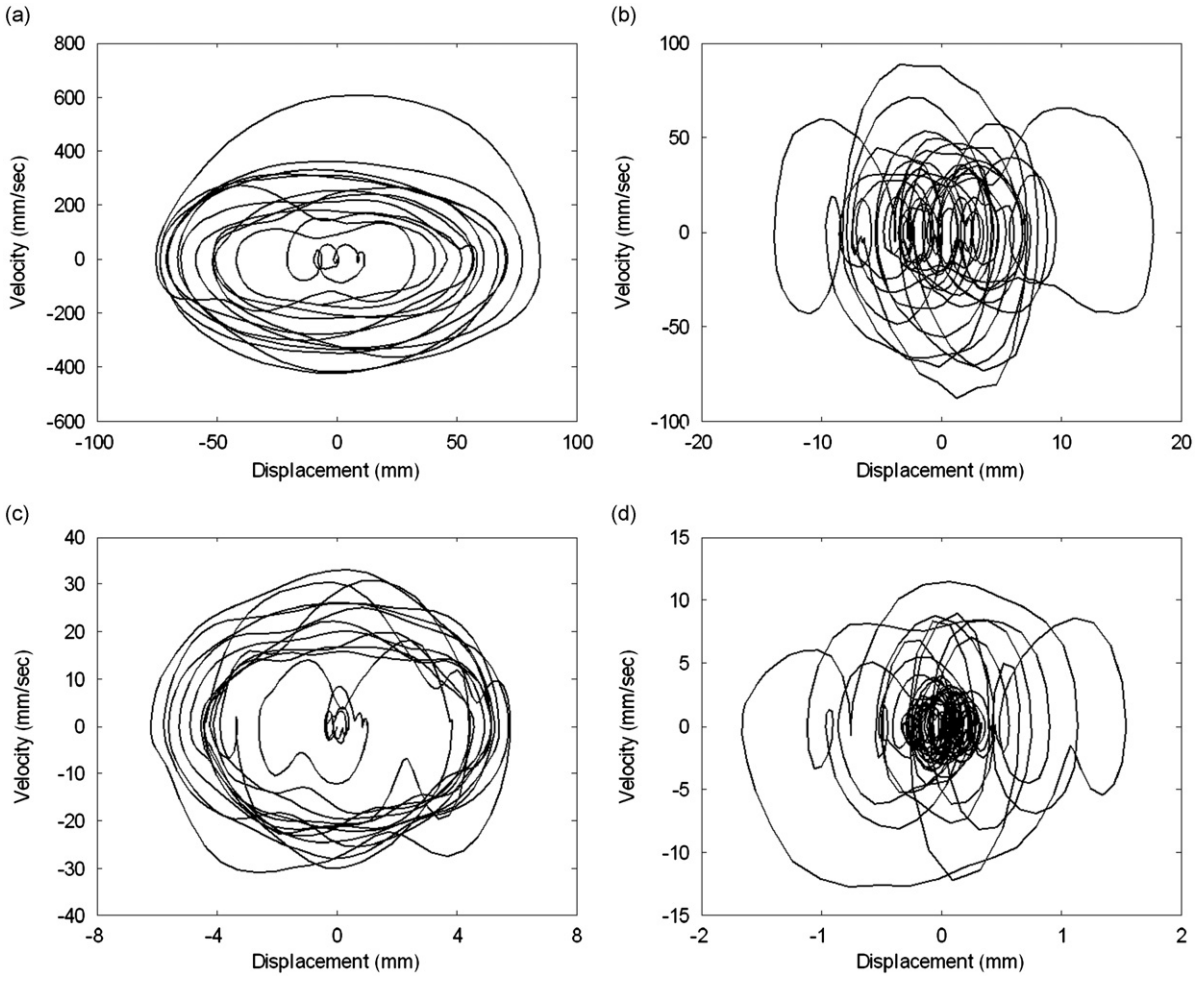

Fig. 7. Optimal polynomial control of nonlinear random oscillators: phase-planes of the PC modes of polynomial chaos expansion with/without control: (a) 1st mode without control, (b) 1st mode with control, (c) 15th mode without control and (d) 15th mode with control (APC-II, $\mu=200$).

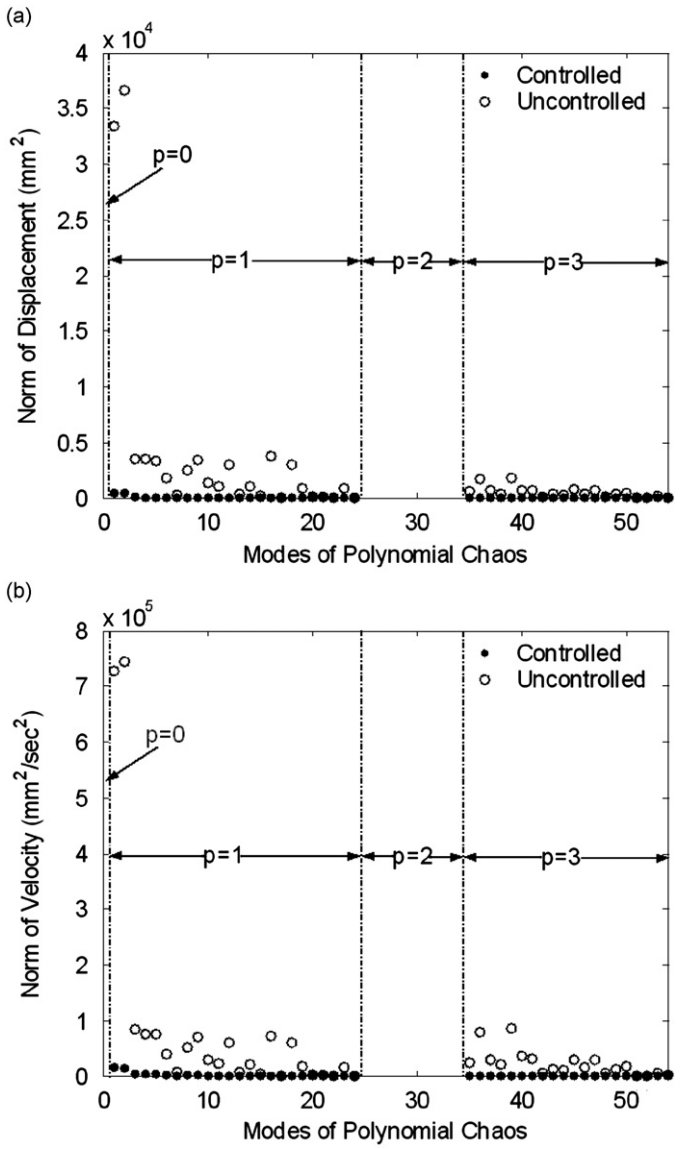

Fig. 8. Optimal polynomial control of nonlinear random oscillators: norm distribution of PC modes of polynomial chaos expansion with/without control: (a) displacement modes and (b) velocity modes (APC-II, $\mu = 200$).

specific nonlinear form of the Duffing oscillator. It is seen from Fig. 8 that the first and second modes of the polynomial chaos expansion (representing the first-order polynomials in the first and second random variables, respectively) of the uncontrolled oscillator are the main contributors to the response, both to displacement and velocity, which reconfirms that the first two random variables contribute most of the fluctuation energy of the responses as shown in Fig. 2. Another remark related to the uncontrolled oscillator is that the higher-orders of homogeneous chaos are significant to the system responses, since the norm of former several modes in the region $p=3$ are bigger than that of some modes in the region $p=1$, indicating that the higher-order modes should be taken into account in the polynomial chaos expansion. It is noted, moreover, that the norms of most PC modes is greatly reduced in the presence of the controller, indicating the value of the proposed stochastic control at managing the uncertainty, in addition to controlling the dynamics of the system.

It is also remarked from Fig. 8 that the extended adaptive procedure where only the cross-terms have been retained [10], tends to under-estimate the solution, in that no all cross-terms have modal energies larger than the energy of monomial terms.

As mentioned previously, the optimal control force is obtained through direct feedback from the system state once the control policy has been determined. Often, the system state is itself the quantity being controlled either to achieve safety, comfort, or serviceability. The optimal control force, itself, however, is often significant for reasons for workability and

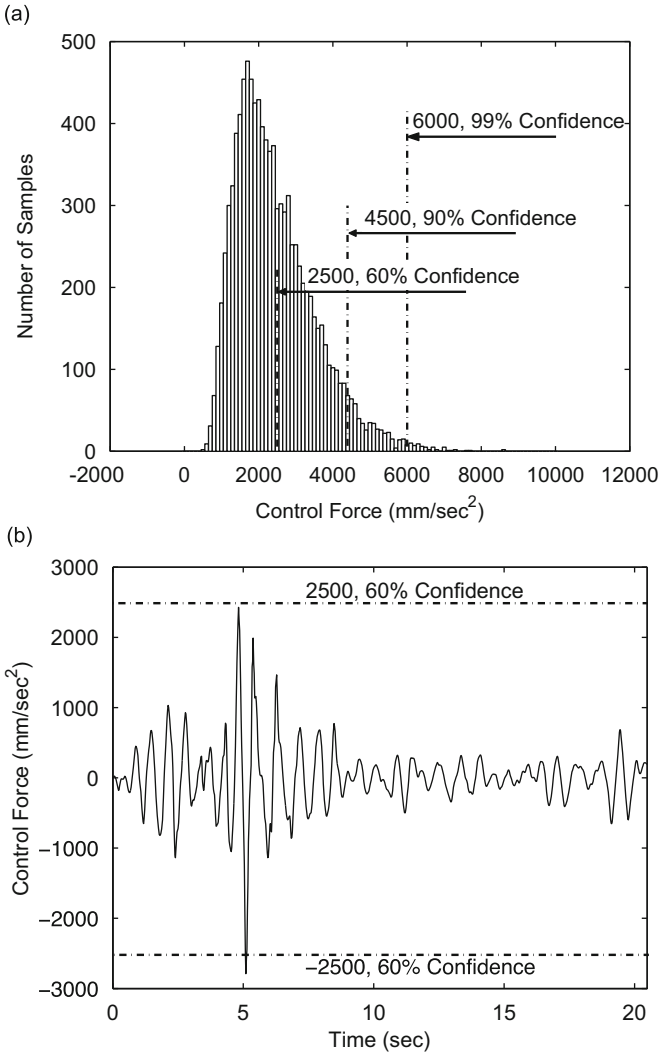

Fig. 9. Optimal polynomial control of nonlinear random oscillators: probabilistic properties of optimal control force on: (a) extreme-value distribution and (b) cross-level of a certain sample process (APC-II, $\mu = 200$).

practicality of the control implementation. A designer might define the specified parameters of the controller according to a probabilistic evaluation of the control force, so as to meet the objective performance of the system. Fig. 9(a) shows the extreme-value distribution of the optimal scaled control force, obtained from a histogram of the maxima over time of the control force associated with 10,000 realizations of the random system. Three crossing-levels are indicated in the figure, together with their confidence levels, 99 percent confidence for level 6000 mm/s^2, 90 percent confidence for level 4500 mm/s^2 and 60 percent confidence for level 2500 mm/s^2 are marked. It is noted that a decision-maker can expediently customize the suitable controller based on a risk analysis. Fig. 9(b) further illustrates the crossing-level of a particular sample process of the optimal control force.

It is noted that, while higher-order PC representations of the dynamics may be required for predictive purposes, a first-order PC expansion seems to be sufficient for the purpose of control. Fig. 10 shows related results associated with a controlled system where a first and third PC expansions have been used. It is of great practical interest to recognize the efficacy of low-order uncertainty representations in the context of adaptive control.

In order to further justify the use of adaptive PC approach in nonlinear control, a comparative study is next carried out with an LQG stochastic optimal control algorithm based on statistical linearization. In this case, the base excitation is modeled as a Gaussian white noise process. Appendix A details the analytical solution of the statistical linearization based LQG, indicating that the quantities of interest are all time-independent. For comparative purpose, the maxima of the root-mean-square quantities of the proposed adaptive control scheme over control interval [0 T] are outlined. Fig. 11 shows the root-mean-square displacements and control forces of the classical optimal control and the adaptive control scheme with

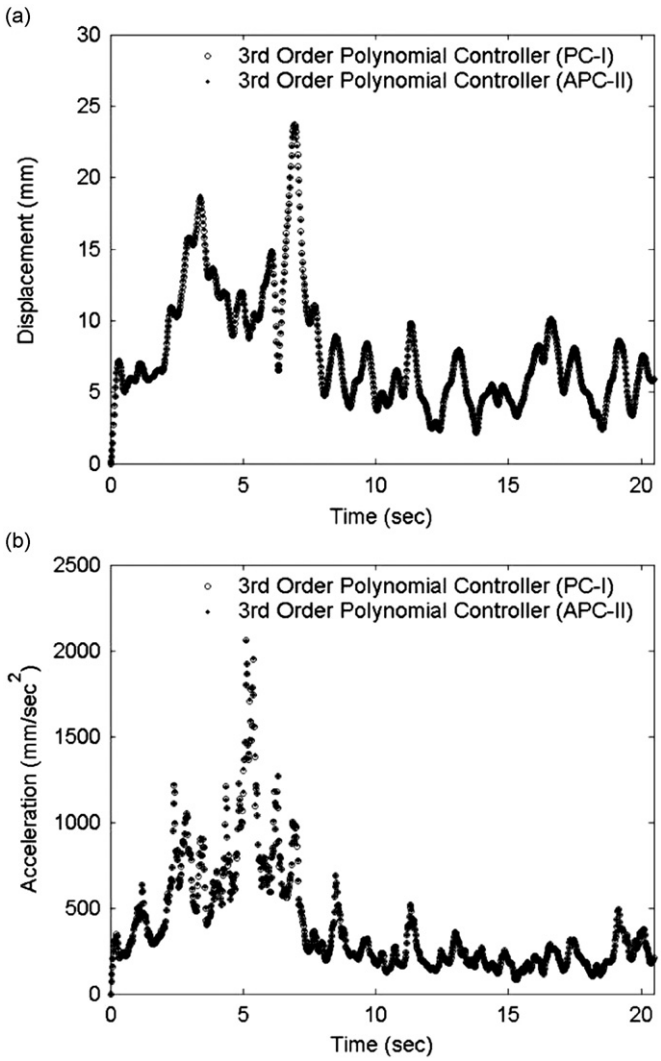

Fig. 10. Optimal polynomial control of nonlinear random oscillators: comparison of time histories of root-mean-square responses of Duffing oscillator using polynomial chaos expansions on: (a) relative displacement and (b) absolute acceleration ($\mu = 200$, PC-I and APC-II refer to the first-order and the third-order PC expansion, respectively).

different nonlinearity levels. It is remarked that the adaptive control scheme behaves better than the LQG using the same weighting matrices. Furthermore, it is noted that the results from the PC approach are insensitive to the strength of nonlinearity of the Duffing oscillator, although the PC approach requires a larger control force. The controller designed by the LQG, however, is sensitive to the strength of nonlinearity of the Duffing oscillator using the present weighting matrices, which has a level-dependent displacement. The displacement of the LQG would be controlled to a lower level than that of the adaptive control scheme if the control weighting matrix **R** is adjusted to 0.1, and the corresponding controller is insensitive to the nonlinear levels, while the control requirement of the LQG is less than that of the adaptive control scheme. It is implied that the LQG underestimates the control requirements, and does not fit the structural control design of civil engineering.

Fig. 12 shows the time histories of root-mean-square responses of a random oscillator with nonlinearity level $\mu = 10$. It can be seen that the relative displacement is greatly reduced by the control action, with a corresponding increase in system acceleration. It is noted that the amount by which the uncontrolled nonlinear system filters acceleration signals depends greatly on the level of nonlinearity. The effect of nonlinearity on this filtering action is weakened significantly following the introduction of the control force. One might, moreover, see that the time histories of root-mean-square responses of the controlled systems with different level of nonlinearity are nearly identical (compare Figs. 4 and 12). It is reconfirmed that the controller designed as PC approach is insensitive to the strength of nonlinearity of the Duffing oscillator.

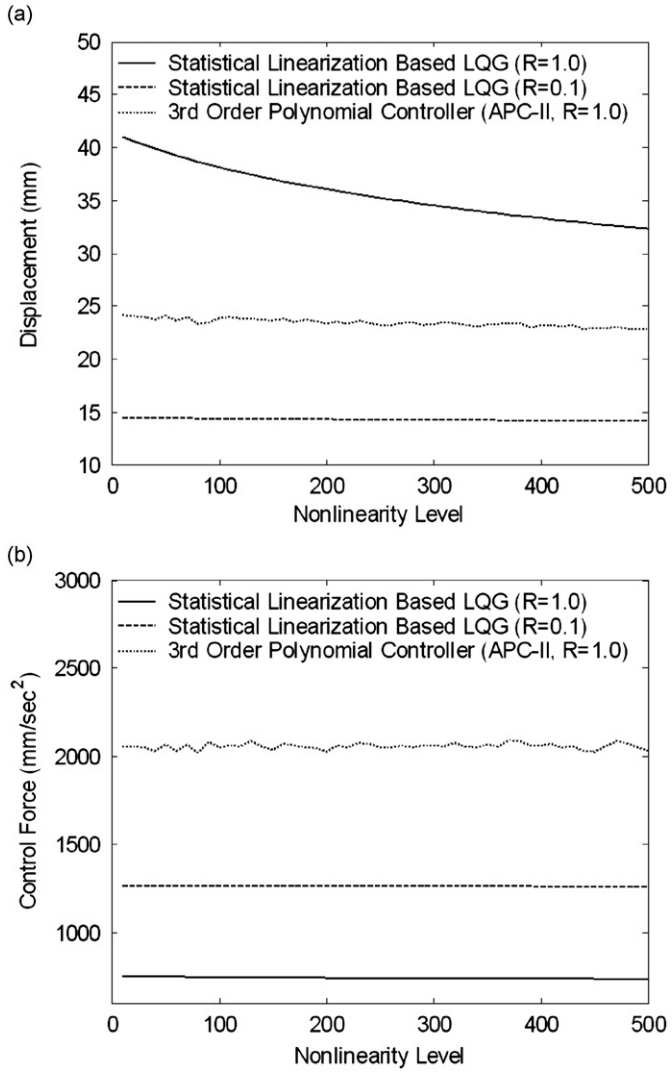

Fig. 11. Optimal polynomial control of nonlinear random oscillators: comparison between root-mean-square quantities of the classical optimal control and extreme values of those using APC-II with different nonlinear levels on: (a) relative displacement and (b) control force.

6. Concluding remarks

The polynomial chaos expansion is introduced into the optimal polynomial control of nonlinear random base-excited oscillators. A discrete representation, the Karhunen–Loeve expansion is employed to represent the physical stochastic ground motion model for the convenient integration with the polynomial chaos expansion. The represented earthquake ground motion is assumed to be a Gaussian non-stationary process with the correlation function of the physical seismic process, which could be viewed as a certain projection of the physical vector space into the Gaussian vector space. An updated scheme of adaptive polynomial chaos is proposed based on a displacement–velocity norm for catching phase orbits of oscillators, which provides an improvement over previous adaptation schemes. Then, an approximate polynomial chaos expansion for the optimal polynomial controller is developed, by which the statistics of quantities of interest can be readily calculated. Numerical investigations are carried out employing the polynomial chaos expansions and the control policy based on Lyapunov asymptotic stability condition. The results reveal that the performance of the Duffing oscillator is improved greatly after controlled, as indicated by various probabilistic quantities of interest. The expansion in first-order homogeneous chaos is observed to be efficient for the design of the polynomial controllers. A further comparative study goes to the controlled nonlinear oscillators using the classical stochastic optimal control, i.e. statistical linearization based LQG being employed to design the optimal controller. It is remarked that the proposed polynomial chaos expansion is a preferred approach to the optimal control of nonlinear random oscillators.

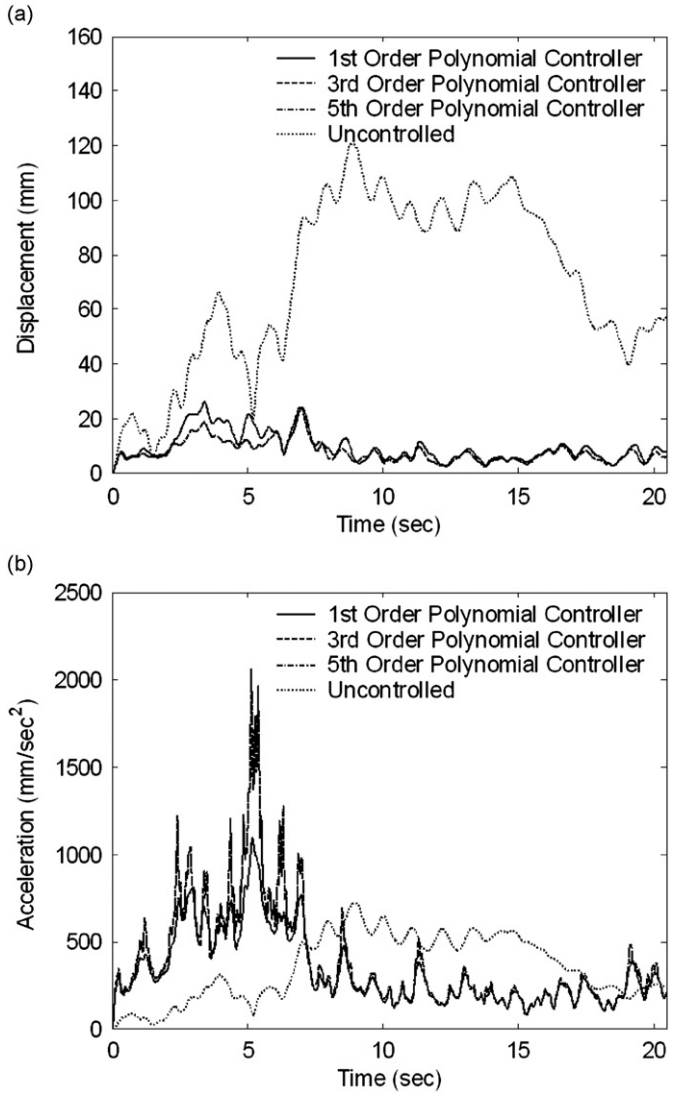

Fig. 12. Optimal polynomial control of nonlinear random oscillators: time histories of root-mean-square responses of Duffing oscillator with/without control: (a) relative displacement and (b) absolute acceleration (APC-II, $\mu = 10$).

Acknowledgements

The support of the National Natural Science Foundation of China for Innovative Research Groups (Grant no. 50621062) is greatly appreciated. The financial support of the China Scholarship Council for the first author's visiting the University of Southern California as a joint Ph.D. student is gratefully acknowledged. Furthermore, the financial support of NSF and AFOSR is acknowledged.

Appendix A. Statistical linearization based LQG control of Duffing oscillators

As a substitute for Eq. (11), the equivalent linear system equation is given by

$$\ddot{x}(t)+2\zeta\omega_0\dot{x}(t)+\omega_{eq}^2 x(t)=u(t)-\ddot{x}_g(\boldsymbol{\Theta},t), \quad x(t_0)=\dot{x}(t_0)=0, \tag{A.1}$$

where ω_{eq} is the natural frequency of the equivalent linear oscillator, obtained by minimizing the expected value of the difference between Eqs. (11) and (A.1) in a least-square sense, i.e.,

$$\frac{\mathrm{d}}{\mathrm{d}\omega_{eq}^2}\langle\{\omega_0^2[x(t)+\mu x^3(t)]-\omega_{eq}^2 x(t)\}^2\rangle=0, \tag{A.2}$$

Then, it yields

$$\omega_{eq}^2 = \omega_0^2\left(1+\mu\frac{\langle x^4(t)\rangle}{\langle x^2(t)\rangle}\right), \tag{A.3}$$

It is seen that ω_{eq} depends on the former fourth-order statistical moments of $x(t)$, the exact evaluation of ω_{eq}^2, thus, requires a knowledge of the probability density function of $x(t)$. As an approximation to the exact solution, the process $x(t)$ might be assumed to be Gaussian [31], and Eq. (A.3) could be simplified as

$$\omega_{eq}^2 = \omega_0^2[1+3\mu\langle x^2(t)\rangle]. \tag{A.4}$$

Here, a decomposition formula has been used for a Gaussian vector $\boldsymbol{\eta}$ [32]:

$$\langle f(\boldsymbol{\eta})\boldsymbol{\eta}\rangle = \langle \boldsymbol{\eta}\boldsymbol{\eta}^{\mathrm{T}}\rangle\langle \nabla f(\boldsymbol{\eta})\rangle. \tag{A.5}$$

where ∇ is the gradient operator defined by

$$\nabla = \left[\frac{\partial}{\partial\eta_1}, \frac{\partial}{\partial\eta_2}, \cdots, \frac{\partial}{\partial\eta_n}\right]^{\mathrm{T}}. \tag{A.6}$$

In the state space, Eq. (A.1) could be written as

$$\dot{\mathbf{Z}}(t) = \mathbf{A}\mathbf{Z}(t)+\mathbf{B}u(t)+\mathbf{D}\ddot{x}_g(\boldsymbol{\Theta},t), \tag{A.7}$$

where

$$\mathbf{Z}(t) = \begin{bmatrix} x(t) \\ \dot{x}(t)\end{bmatrix}, \quad \mathbf{A} = \begin{bmatrix} 0 & 1 \\ -\omega_{eq}^2 & -2\zeta\omega_0\end{bmatrix}, \quad \mathbf{B} = \begin{bmatrix} 0 \\ 1\end{bmatrix}, \quad \mathbf{D} = \begin{bmatrix} 0 \\ -1\end{bmatrix}. \tag{A.8}$$

A cost function involved in the stochastic linear quadratic regulator problem is considered [33]:

$$J(\mathbf{Z},u,t) = \langle \boldsymbol{S}(\mathbf{Z}(t_f),t_f)+\frac{1}{2}\int_{t_0}^{t_f}[\mathbf{Z}^{\mathrm{T}}(t)\mathbf{Q}\mathbf{Z}(t)+\mathbf{R}u^2(t)]\,\mathrm{d}t\rangle, \tag{A.9}$$

subjected to

$$d\mathbf{Z}(t) = [\boldsymbol{A}\mathbf{Z}(t)+\mathbf{B}u(t)]\,\mathrm{d}t+\mathbf{L}\,\mathrm{d}W(t), \quad \mathbf{Z}(t_0)=\mathbf{0}. \tag{A.10}$$

where $\mathbf{L}$ is the (2×1) force influence matrix; $W(t)$ is a one-dimensional Brownian motion process modeled by a Gaussian white noise with

$$\langle \mathrm{d}W(t)\rangle = 0, \quad \langle \mathrm{d}W^2(t)\rangle = 2\pi S_0\,\mathrm{d}t. \tag{A.11}$$

Eq. (A.10) is a Ito stochastic differential equation, the mathematical representation of the Duffing system equation (A.7), indicating that the assumption of the measure noise on $\mathbf{Z}(t)$,$u(t)$ are both ignored, and the external stochastic excitation $\ddot{x}_g(\boldsymbol{\Theta},t)$ ideally modeled by the white noise. It is noted that S_0 in (A.11) represents the spectral intensity of $\ddot{x}_g(\boldsymbol{\Theta},t)$, defined by [34]

$$S_0 = \frac{\overline{a}_{\max}^2}{f^2\omega_e}, \tag{A.12}$$

where $\overline{a}_{\max}$ is the mean of extreme values of ground motions, denoting 0.3g in this investigation; f is the peak factor, which is 3.1 for the site soil of type III. ω_e is the area of unit spectral intensity factor, and the corresponding value is 29.93 rad/s. It is deduced, according to Eq. (A.12), that S_0 is 0.03005 $\mathrm{m}^2/\mathrm{s}^3$.

The minimization of the cost function Eq. (A.9) results in the Hamilton–Jacobi–Bellman equation in stochastic scenario. Introducing the generalized Hamilton equation [35]:

$$H_G\left(\mathbf{Z},u,\frac{\partial}{\partial Z},\frac{\partial^2}{\partial Z^2},t\right) = \frac{1}{2}[\mathbf{Z}^{\mathrm{T}}(t)\mathbf{Q}\mathbf{Z}(t)+\mathbf{R}u^2(t)]+\frac{\partial V}{\partial Z}[\mathbf{A}\mathbf{Z}(t)+\mathbf{B}u(t)]+\pi S_0\left(\frac{\partial^2 V}{\partial Z^2}\mathbf{L}\mathbf{L}^{\mathrm{T}}\right). \tag{A.13}$$

where $V = V(\mathbf{Z},t)$ is the optimal cost function, assumed as the following form [35]:

$$V(\mathbf{Z},t) = \tfrac{1}{2}[\mathbf{Z}^{\mathrm{T}}(t)\mathbf{P}(t)\mathbf{Z}(t)+v(t), \tag{A.14}$$

where $v(t)$ is a correction term due to randomness inherent in the generalized Hamiltonian function compared with the deterministic counterpart. According to the variation principle, we have

$$u(t) = -\mathbf{R}^{-1}\mathbf{B}^{\mathrm{T}}\mathbf{P}\mathbf{Z}(t), \tag{A.15}$$

$$v(t) = \pi S_0\int_{t_0}^{t_f}\mathrm{tr}(\mathbf{P}(\boldsymbol{t})\mathbf{L}\mathbf{L}^{\mathrm{T}})\,\mathrm{d}t. \tag{A.16}$$

where $\mathbf{P}(t)$ can be approximately as $\mathbf{P}$, satisfying the following Riccati matrix algebraic equation:

$$\mathbf{PA}+\mathbf{A}^{\mathrm{T}}\mathbf{P}-\mathbf{PBR}^{-1}\mathbf{B}^{\mathrm{T}}\mathbf{P}+\mathbf{Q}=\mathbf{0}. \tag{A.17}$$

It is remarked that the control gain matrix of the LQG control is identical to that of the classical determinate LQR control with closed-loop means, indicating that for the Gaussian white noise driven linear systems, the control gain matrix can be computed off-line. The Riccati matrix $\mathbf{P}$ hinges on $\langle x^2(t)\rangle$ due to ω_{eq} locating in the system matrix $\mathbf{A}$, which demands the control gain computed on-line. Also, $\mathbf{P}$ can be calculated approximately at the initial state $\mathbf{Z}(t_0)=\mathbf{0}$, where $\omega_{eq}^2=\omega_0^2$ referring to (A.4).

Taking Eq. (A.15) into Eq. (A.1) and using Fourier transform, we have

$$\{[(\omega_{eq}^2+\overline{K})-\omega^2]+(2\zeta\omega_0+\overline{C})(\mathrm{i}\omega)\}x(\omega)=-\ddot{x}_g(\boldsymbol{\Theta},\omega), \tag{A.18}$$

where $\overline{C},\overline{K}$ are the numerical damping and numerical stiffness provided by the optimal control $u(t)$, respectively,

$$\overline{C}=\mathbf{R}^{-1}(B_1P_{12}+B_2P_{22}),\quad \overline{K}=\mathbf{R}^{-1}(B_1P_{11}+B_2P_{21}). \tag{A.19}$$

Further, the mean-square displacement is deduced as

$$\langle x^2(t)\rangle=\int_{-\infty}^{\infty}\frac{S_0}{[(\omega_{eq}^2+\overline{K})-\omega^2]^2+(2\zeta\omega_0+\overline{C})^2\omega^2}\mathrm{d}\omega. \tag{A.20}$$

The closed solution of Eq. (A.20) can be attained as a specific rule [31], i.e.,

$$\langle x^2(t)\rangle=\frac{\pi S_0}{(\omega_{eq}^2+\overline{K})(2\zeta\omega_0+\overline{C})}. \tag{A.21}$$

Taking account for Eq. (A.4), a single algebraic equation for $\langle x^2(t)\rangle$ appears

$$\langle x^2(t)\rangle=\frac{\sqrt{(\omega_0^2+\overline{K})^2+\dfrac{12\pi\mu\omega_0^2S_0}{2\zeta\omega_0+\overline{C}}}-(\omega_0^2+\overline{K})}{6\mu\omega_0^2}. \tag{A.22}$$

The relationship between the state and the control force in frequency domain is

$$u(\omega)=[-\overline{C}(\mathrm{i}\omega)-\overline{K}]x(\omega), \tag{A.23}$$

and the mean-square control force is deduced as

$$\langle u^2(t)\rangle=\int_{-\infty}^{\infty}\frac{(\overline{K}^2+\overline{C}^2\omega^2)S_0}{[(\omega_{eq}^2+\overline{K})-\omega^2]^2+(2\zeta\omega_0+\overline{C})^2\omega^2}\mathrm{d}\omega, \tag{A.24}$$

Likewise, we have the closed solution of the mean-square control force

$$\langle u^2(t)\rangle=\frac{\pi S_0\overline{C}^2}{2\zeta\omega_0+\overline{C}}+\frac{\left[\sqrt{(\omega_0^2+\overline{K})^2+\dfrac{12\pi\mu\omega_0^2S_0}{2\zeta\omega_0+\overline{C}}}-(\omega_0^2+\overline{K})\right]\overline{K}^2}{6\mu\omega_0^2}. \tag{A.25}$$

References

[1] N. Wiener, The homogeneous chaos, *American Journal of Mathematics* 60 (1938) 897–936.
[2] R.H. Cameron, W.T. Martin, The orthogonal development of nonlinear functionals in series of Fourier–Hermite functionals, *Annals of Mathematics* 48 (1947) 385–392.
[3] R. Ghanem, P. Spanos, *Stochastic Finite Elements: A Spectral Approach*, Springer, New York, 1991.
[4] R. Ghanem, Stochastic finite elements for heterogeneous media with multiple random non-Gaussian properties, *ASCE Journal of Engineering Mechanics* 125 (1999) 26–40.
[5] R. Ghanem, Ingredients for a general purpose stochastic finite element formulation, *Computer Methods in Applied Mechanics and Engineering* 168 (1999) 19–34.
[6] O.P. Le Maitre, H. Najm, R. Ghanem, O. Knio, Multiresolution analysis of Wiener-type uncertainty propagation schemes, *Journal of Computational Physics* 197 (2004) 502–531.
[7] D. Xiu, G. Em Karniadakis, The Wiener–Askey polynomial chaos for stochastic differential equations, *SIAM Journal on Scientific Computing* 24 (2002) 619–644.
[8] R. Li, R. Ghanem, Adaptive polynomial chaos expansions applied to statistics of extremes in nonlinear random vibration, *Probabilistic Engineering Mechanics* 13 (1998) 125–136.
[9] A. Doostan, R. Ghanem, J. Red Horse, Stochastic model reduction for chaos representations, *Computer Methods in Applied Mechanics and Engineering* 196 (2007) 3951–3966.
[10] D. Lucor, G.E. Karniadakis, Adaptive generalized polynomial chaos for nonlinear random oscillators, *SIAM Journal on Scientific Computing* 26 (2004) 720–735.
[11] A. Monti, F. Ponci, T. Lovett, A polynomial chaos theory approach to the control design of a power converter, in: *Proceedings of 350th Annual IEEE Power Electronics Specialists Conference*, Aachen, 2004, pp. 4809–4813.
[12] F.S. Hover, M.S. Triantafyllou, Application of polynomial chaos in stability and control, *Automatica* 42 (2006) 789–795.
[13] J. Suhardjo Jr., B.F. Spencer, M.K. Sain, Nonlinear optimal control of a duffing system, *International Journal of NonLinear Mechanics* 27 (1992) 157–172.
[14] D.S. Bernstein, Nonquadratic cost and nonlinear feedback control, *International Journal of Robust and Nonlinear Control* 3 (1993) 211–229.

[15] A. Agrawal, J.N. Yang, J.C. Wu, Non-linear control strategies for duffing systems, *International Journal of Non-Linear Mechanics* 33 (1998) 829–841.
[16] J.B. Chen, W.Q. Liu, Y.B. Peng, J. Li, Stochastic seismic response and reliability analysis of base-isolated structures, *Journal of Earthquake Engineering* 11 (2007) 903–924.
[17] S. Das, R. Ghanem, S. Finette, Polynomial chaos representation of spatio-temporal random fields from experimental measurements, *Journal of Computational Physics* 228 (2009) 8726–8751.
[18] J.B. Chen, J. Li, A note on the principle of preservation of probability and probability density evolution equation, *Probabilistic Engineering Mechanics* 24 (2009) 51–59.
[19] J. Li, Y.B. Peng, J.B. Chen, A physical approach to structural stochastic optimal controls, *Probabilistic Engineering Mechanics* 25 (2010) 127–141.
[20] B.D.O. Anderson, J. Moore, *Optimal Control: Linear Quadratic Methods*, Prentice-Hall International Editions, New Jersey, 1990.
[21] J.N. Yang, A.K. Agrawal, S. Chen, Optimal polynomial control for seismically excited nonlinear and hysteretic structures, *Earthquake Engineering and Structural Dynamics* 25 (1996) 1211–1230.
[22] R.E. Kalman, Contribution to the theory of optimal control, *Boletin de la Sociedad Matematica Mexicana* 5 (1960) 102–119.
[23] M.K. Sain, Control of linear systems according to the minimal variance criterion-a new approach to the disturbance problem, *IEEE Transactions on Automatic Control* (1966) 118–122.
[24] R.F. Stengel, L.R. Ray, C.I. Marrison, Probabilistic evaluation of control system robustness, *IMA Workshop on Control Systems Design for Advanced Engineering Systems: Complexity, Uncertainty, Information and Organization*, Minneapolis, October 12–16, 1966.
[25] B.F. Spencer Jr., D.C. Kaspari Jr., M.K. Sain, Structural control design: a reliability-based approach, in: *Proceedings of the American Control Conference*, Baltimore, 1966, pp. 1062–1066.
[26] B.S. May, J.L. Beck, Probabilistic control for the active mass driver benchmark structural model, *Earthquake Engineering and Structural Dynamics* 27 (1998) 1331–1346.
[27] W.Q. Zhu, Z.G. Ying, T.T. Soong, An optimal nonlinear feedback control strategy for randomly excited structural systems, *Nonlinear Dynamics* 24 (2001) 31–51.
[28] R.V. Field, L.A. Bergman, Reliability-based approach to linear covariance control design, *Journal of Engineering Mechanics* 124 (1998) 193–199.
[29] O. Elbeyli, L. Hong, J.Q. Sun, On the feedback control of stochastic systems tracking prespecified probability density functions, *Transactions of the Institute of Measurement and Control* 27 (2005) 319–329.
[30] J.N. Yang, Z. Li, S.C. Liu, Stable controllers for instantaneous optimal control, *ASCE Journal of Engineering Mechanics* 118 (1992) 1612–1630.
[31] J.B. Roberts, P.D. Spanos, *Random Vibration and Statistical Linearization*, John Wiley & Sons, Chichester, 1990.
[32] I.E. Kazakov, Generalization of the method of statistical linearization to multidimensional systems, *Automation and Remote Control* 26 (1965) 1201–1206.
[33] S.P. Chen, X.J. Li, X.Y. Zhou, Stochastic linear quadratic regulators with indefinite control weight costs, *SIAM Journal on Control and Optimization* 36 (1998) 1685–1702.
[34] F. Hong, J.R. Jiang, Y.T. Li, Power spectral models of earthquake ground motions and valuation of its parameters, *Earthquake Engineering and Engineering Vibration* 14 (1994) 46–51.
[35] J. Li, J.B. Chen, *Stochastic Dynamics of Structures*, John Wiley & Sons, Singapore, 2009.